Chemical Physics Letters 640 (2015) 201–214

Contents lists available at ScienceDirect

Chemical Physics Letters

journal homepage: www.elsevier.com/locate/cplett

Comparison of degradation mechanisms in organic photovoltaic devices upon exposure to a temperate and a subequatorial climate

Vianou Irénée Madogni[a,b,*], Basile Kounouhéwa[a,b], Aristide Akpo[a,b], Macaire Agbomahéna[c], Saliou Amoussa Hounkpatin[a,b], Cossi Norbert Awanou[a,b]

[a] Département de Physique (FAST) et "Ecole Doctorale Sciences des Matériaux (EDSM)", Université d'Abomey-Calavi, Benin
[b] Laboratoire de Physique du Rayonnement LPR, FAST-UAC, 01BP 526 Cotonou, Benin
[c] Laboratoire de Caractérisation Thermophysique des Matériaux et Appropriation Energétique (Labo CTMAE/EPAC/UAC), Abomey-Calavi, Benin

ARTICLE INFO

Article history:
Received 20 July 2015
In final form 13 September 2015
Available online 23 October 2015

ABSTRACT

We compared the degradation process in organic bulk heterojunction solar cells, upon exposure to a temperate (Belgium) and a sub-equatorial (Benin) climate. Differences in degradation of these devices have been attributed to humidity differences between the temperate and Beninese environments.

Our analyses revealed, the decrease rate on 240 h of J_{SC} is about 40% in Belgium and 45% in Benin, when the devices are exposed to light and to ambient air. The diffusion of H_2O and O_2 species through the layers is more rapid when the temperature is high.

1. Introduction

Solar cells have in last decades established their importance as an eco-friendly, sustainable energy source. Organic solar cells, in specific, are low-cost, highly scalable, flexible, light-weight, with a short energy payback time, and consequently of high commercial interest [1]. Still, improving the lifetime of the devices remains a serious issue that has to be resolved in order to make them commercially feasible. The energy efficiency of these organic solar cells has significantly increased in recent years. This energy conversion efficiency of about 10.7% obtained by Green et al. [2], reached a record of 12% recently, obtained on a standard size of 1:1 cm^2 combining two different absorbent materials [3]. But these organic solar cells, still know many degradation processes due to their exposure to oxygen, humidity, temperature, atmospheric pressure, and long time ultraviolet (UV) illumination [4,5]; which makes the intrinsic lifetime of the devices without encapsulation very short [6]. The limited lifetime is a result of several processes that are in play simultaneously.

Known degradation mechanisms involve: diffusion of molecular oxygen and water into the device, degradation of interfaces, degradation of the active material, inter-layer and electrode diffusion, electrode reaction with the organic materials, morphological changes, and macroscopic changes such as delamination, formation of particles, bubbles, and cracks [7]. Some of these degradation mechanisms are interrelated and take place at the same time, some during operation of the solar cell, and some during storage. Some degradation mechanisms are fast, and others are slow. It is thus a challenging task to identify degradations mechanisms, and even more difficult to quantify to what extent each mechanism contributes to the overall deterioration of the solar cell performance [8]. Earlier works have shown that, for normal geometry devices using aluminum as a back electrode, both molecular oxygen and water will diffuse through the aluminum electrode [8–10]. The spatial distribution of reaction products in multilayer polymer solar cells induced by water and oxygen atmospheres has been mapped and used to elucidate the degradation patterns and failure mechanisms in an inverted polymer solar cell [11]. A comparison has been made between the use of a humid (oxygen-free) atmosphere and a dry oxygen atmosphere during testing of devices that were kept in the dark and devices that were subjected to illumination under simulated sunlight. They have found that the reactions taking place at the interface between the active layer and the PEDOT:PSS were the major cause of device failure in the case of these inverted devices, which are compatible with full roll-to-roll (R2R) coating and industrial manufacture. The PEDOT:PSS has been found to phase separate, with the PEDOT-rich phase being responsible for most of the interface degradation in oxygen atmospheres. In water atmospheres, little chemically induced degradation has been observed, whereas a large partially reversible dependence of the open circuit voltage on the relative humidity has been observed. All organic layers will react with molecular oxygen and water in varying degree causing oxidation and thus degradation. At the ITO

* Corresponding author at: Département de Physique (FAST) et Ecole Doctorale Sciences des Matériaux (EDSM), Université d'Abomey-Calavi, Benin.
E-mail address: ivianou@yahoo.fr (V.I. Madogni).

http://dx.doi.org/10.1016/j.cplett.2015.09.023

interface, oxygen from the ITO will be exchanged with the incoming oxygen (i.e., in the form of molecular oxygen and water). These processes are in varying degree affected by light and/or heat [10,11].

Light is then one of the main triggers for polymers degradation. Photochemical degradation affects the electronic properties, photo-conductive, mechanics and causes a photo-decrease of the material [1,10–12]. The photochemical degradation of π-conjugated polymers and the impact of this degradation on the performances of the organic solar cells have been the subject of many studies [1,12–21], etc., in particular, many experimental works have been done to investigate the underlying mechanism of the P3HT photochemical degradation in organic bulk heterojunction solar cells [22]. The most studied polymer solar cell employs morphologically stable bulk heterojunctions, regioregular P3HT (rrP3HT) as the donor material and the fullerene (PCBM) as the acceptor material. Previously it was believed that the chemical reaction responsible for its degradation was direct attack on the thiophene ring by singlet oxygen, but instead it has been shown to be a side chain oxidation starting with a hydroperoxide formation at the benzylic position [19,23]. Films of P3HT are photo-oxidized fairly rapidly with complete bleaching after 700 h depending on thickness. Adding PCBM slows this process considerably, presumably by sub nanosecond quenching the reactive excited state on P3HT forming a lower energy charge transfer complex [24]. Reese et al. concluded that oxidation of PCBM, creating species with up to eight oxygen atoms, formed traps for the electron transport decreasing the electron mobility [25]. Schafferhans et al. similarly investigated the effect of oxygen doping of P3HT:PCBM blends and concluded that exposure to O_2 in the dark resulted in a loss of J_{SC} while all solar cell parameters were affected in light, all due to increased number of oxygen generated trap states [26]. This is also in line with a previous study by Seemann et al. on the influence of oxygen on organic solar cells with gas permeable electrodes [27]. The reaction between P3HT and oxygen may be initiated with an initial reversible formation of one or more meta-stable charge transfer states [28,29]. Several studies showed that charges have been formed when P3HT:PCBM has been illuminated and exposed to oxygen. This charge build-up could be reversed in vacuum indicating a weak ($P3HT^+:O_2$) complex. Recent studies carried out with the analogous polymer poly-(3-octyl-thiophene) (P3OT) by Abad et al. concludes that the degradation mechanism involves UV-initiated ozone formation and that ozone is the reactive species responsible for the P3OT degradation [30,31].

Seemann et al. [32] studied degradation behavior of an inverted device similar to the one described in [11]. They found that due to the gas permeability of the PEDOT:PSS, oxygen can diffuse through, which, combined with illumination, results in a strong decrease of the short-circuit current (within minutes). The authors explain the decrease from a change in the conductivity of the PEDOT:PSS layer and they found that the short circuit current can be partially recovered by heating, which they take as an indication of degradation taking place in the photoactive layer. Yamanari et al. studied the effect of PEDOT:PSS in a normal geometry device with respect to degradation [33]. It was found that when PEDOT:PSS is used degradation is fast as compared to either no PEDOT:PSS or using MoO_x instead of PEDOT:PSS. They showed that PEDOT:PSS accelerates the formation of aluminum oxide in the interface between the aluminum electrode and the active layer.

As solar cells are multi-layered structures, the decay in their performance reflects not only the degradation of the photo-active layer, but of each of its constituent layers [1]. In contact with air and light, the polymer reacts with oxygen, which produces different oxidized polymer species and breaks the polymer chain, leading to irreversible failure in functioning of the devices [19,34–38]. Recently Hintz et al. have shown that, two concurrent mechanisms take place in degradation process, depending on the irradiation conditions [39,40]. Under the UV irradiation, the degradation proceeds as a radical reaction [19,34,36,37] starting at the α-carbon of the alkyl side chain, and results with simultaneous degradation of the conjugated system and the side chain. Under visible illumination, however, the reaction involves a photosensitized species, possibly singlet oxygen that primarily destroys the π-conjugated system of the polymer, leaving the side chain almost unaffected [41–45]. In white light conditions, both of the mechanisms are active, but since the radical chain mechanism has a higher effectiveness, it dominates even when only a low UV irradiation fraction is present [39,40]. Besides the irreversible degradation mechanisms, an additional reversible process takes place. It was reported the first time by Abdou et al. that when exposed to oxygen and light, P3HT gets reversibly doped via a polymer-oxygen charge transfer complex [44]. This finding has been later confirmed by many other groups [15,26,29,46,47].

The objective of this letter is to compare the degradation process of the organic bulk heterojunction devices: ITO/PE-DOT:PSS/rrP3HT:PC70BM (1:0.7 weight ratio)/Yb/Al, upon exposure to a temperate (Belgium) and a sub-equatorial (Benin) climate from the experimental data that we dispose. Differences in the degradation process have been studied. The weak performance observed in time for these devices, in terms of electrodes degradation, interfaces and the charge transport mechanism have been analyzed and interpreted. Moreover, the degradation mechanism analysis of these devices under the Beninese climate, fits into the overall approach to the development of new kits or sunlamps, for people who have not access to conventional electricity, but lying in areas under strong solar illumination especially in undeveloped countries. We can quote in this context the program 'Lighting for Africa' [48] which supports the development of a prototype of solar lights tested in Zimbabwe or the project 'Eight19' [49] which elaborates the solar lights with a battery charging system.

The letter is organized as follows: in Section 2, the architecture of the organic bulk heterojunction solar cell considered is described. Subsequently, link causes–effect of degradation, degradation of the hole transport layer, degradation of the metal electrode, photo-oxidation of the active layer, degradation by oxygen and water molecules, effect of the atmosphere, parameters affect and the possible causes, physical stability of the solar cells are presented and interpreted. The results and discussion are presented in Section 3. Finally, the conclusion and outlook are listed in Section 4.

2. Materials and methods

2.1. Architecture of the organic solar cell

The structure of the solar cell considered, is blend of ITO/PEDOT:PSS/rrP3HT:PC70BM (1:0.7 weight ratio)/Yb/Al. The layer Yb/Al is cathode and ITO/PEDOT:PSS is anode. The ITO (85 nm) layer on glass is a transparent semi-conductor and serves of anode in the structure. It collects the holes after the separation of excitons and the charges transport. It is composed a blend of 90% indium oxide (In_2O_3) and 10% of tin oxide (SnO_2). The ITO electrodes are covered with a film of PEDOT:PSS (40 nm) deposited by spin-coating from an aqueous solution. The PEDOT:PSS layer collects the holes and limits the electrochemistry between the active layer and the anode. It decreases the roughness of the ITO surface. PEDOT favors the holes transport but presents the drawback of being hydrophilic. rrP3HT:PC70BM (1:0.7 weight ratio) (100 nm) is the active layer; it is the seat of the charge photogeneration. PC70BM is a good electron acceptor; it presents a great chemical stability and good charge mobility. rrP3HT is the electron donor, it presents good electrical properties (good mobility of the charge carriers), good optical properties and an appreciable chemical stability

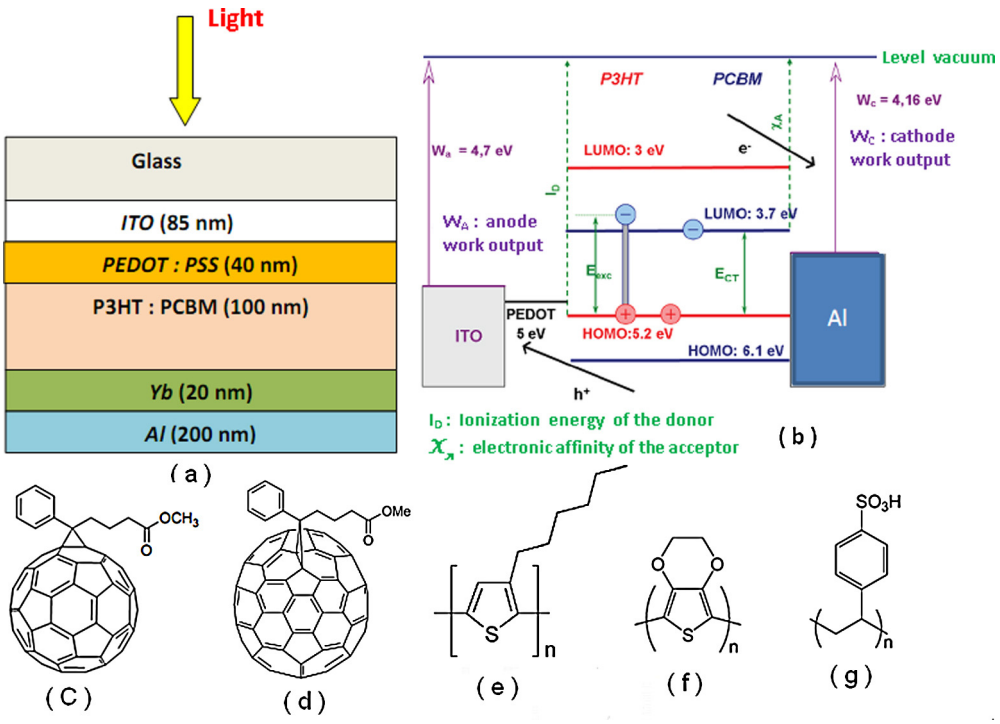

Figure 1. (a) Ideal structure of the cell, (b) band diagram of the cell ITO/PE DOT/rrP3HT:PCBM/Yb/Al proposed by our work, (C) [6,6]-phenyl C61-butyric acid methyl ester (PCBM), (d) methano-fullerene-[6,6]-phenyl-C71 methyl butyrate (PC70BM), (e) regioregular poly(3-hexylthiophene), (f) poly (3, 4-ethylenedioxythiophene) (PEDOT), (g) poly (styrenesulfonate) (PSS) [53].

for manufacturing of the organic photovoltaic devices. The Al/Yb layer collects the electrons and the aluminum (Al (200 nm)) layer presents a great surface roughness. Ytterbium (20 nm) layer limits its electrochemistry between aluminum (Al) and sulfur of rrP3HT in film and allows improvement of open circuit voltage, shunt resistance and fill factor (FF). Ytterbium (Yb) forms a barrier layer between the active layer and aluminum (Al) [50].

The BHJ blend is represented by the HOMO and LUMO levels of the donor and acceptor. The band offset between the LUMO levels of donor and acceptor guarantees the charge separation at the interface if the lifetime of the exciton is sufficiently long to meet a split site as shown in Figure 1.

The choice of donor–acceptor pair defines the alignment of electronic levels of the system. This alignment is important because the energy difference between the HOMO of the donor and the LUMO of the acceptor is directly linked to the potential V_{OC} of the solar cell while the energy difference between the LUMO of the two materials ensures exciton dissociation [51,52].

The blend rrP3HT:PC70BM is chosen to indicate the interest of complementary absorption of PC70BM in active layer [53].

2.2. Link cause–effect of degradation

Whatever the climatic conditions, we have identified several factors and degradation processes in the literature [10,54–56]: (i) the diffusion of oxygen and water through the layer induces chemical reactions, (ii) direct photo-degradation of the active layer, (iii) thermal degradation of the active layer, (iv) the corrosion to the interfaces of electrodes, (v) the inter-layers diffusion, (vi) chemical defects formation in the active layer. These physical and/or chemical degradation modes of (flexible) OPVs devices can be divided in two main categories: (I) intrinsic degradation due to changes in the characteristics of the interface between layers of the stacking owing to internal modification of the materials used, (II) extrinsic degradation caused by changes in the cell behavior induced by external triggers, such as water, oxygen and electromagnetic radiations (UV, visible light, IR, etc.). The latter is strongly linked to the quality and stability in properties of the encapsulation system, namely the barrier, the substrate and the type of edge sealing used.

We indicated for different external constraints, the consequences on organic photovoltaic cells. We summarized of various failure modes (causes/effect) leading to reduction in efficiency in OPVs (Table 1). Some factors or constraints are inter-dependents. For example, illumination causes an increase of the temperature in the cell. These two factors facilitate the diffusion of the oxygen and water, and therefore the oxidization mechanism. We notice that the elevation of the sole temperature is a factor which also facilitates the diffusion as that has been predicted in the literature. The technique used depends on the objectives attached for the aging study [12]. Generally, the analyses are essentially focused on the active layer degradation by chemical aging under the effect of light or the combination of the light and oxygen. Physical aging by the analysis of the morphological stability on the degradation of the

Table 1
Link cause–effect of degradation: summary of various failure modes (causes/effect) leading to reduction in efficiency in OPVS [57].

Stress	Response
Mechanical	Delamination, electrode failure, packaging failure
Temperature	Acceleration, delamination, morphological changes, diffusion
Light: (spectral/response; total intensity)	Photochemical oxidation, photo bleaching, yellowing, mechanical failure
Oxygen: (humidity/water)	D/A oxidation, electrodeoxidation, charge extraction, charge mobility, TCO etching, interface failure
Coupled-effect (light/mechanical water/mechanical)	Interconnected failure (in addition to above mentioned failure)
Electrical: (electrical field)/(coulombic charges)	Localized heating, shorts

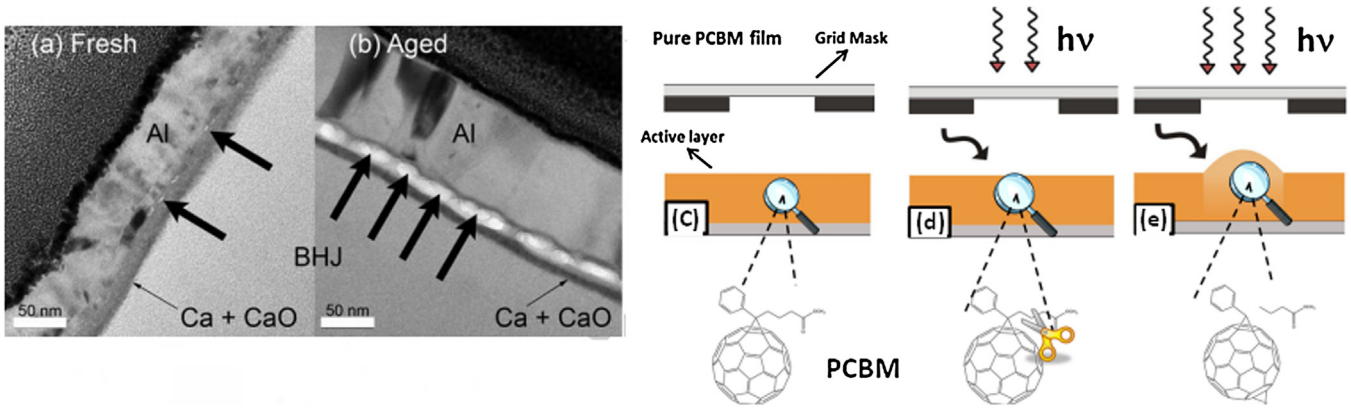

Figure 2. (a) Freshly prepared and (b) aged ITO/BHJ/Ca/Al devices. The active organic region is labeled BHJ, the aluminum layer of the electrode is identified as Al, and the calcium layer, which likely contains a significant fraction of calcium oxide, is labeled Ca + CaO. Bold arrows indicate regions of void formation at the Ca/Al interface that enlarge as the devices age [60]; schematic of the processes inside the pure PCBM sample, (C) a zoom into the active layer shows the intact fullerene structure, (d) In the initial stages of degradation, the side chain of the PCBM is rst lost. This leads to no change in topography. (e) In the next stages, the oxygen gets incorporated in the C60 forming an epoxide structure thereby increasing the layer thickness [53].

electrodes at the interface depends on the nature of the used metal (aluminum, calcium, lithium, etc.), and the transparent conductive oxide, and the degradation study of the encapsulated and the substrate. Our analyses are focused on the active layer rrP3HT:PC70BM (1:0.7 weight ratios), by chemical aging under the effect of the light, light and oxygen and the combination of oxygen and moisture. Physical aging by the analysis of the morphological stability on the degradation of the electrodes at the interface depending on the aluminum used during the exposure test under air and in the dark, in the visible light and the ambient air.

2.3. Degradation of the metal electrode

Certain metals such as Al, Ca and Ag are commonly used as electrodes in OPV devices because of their high electrical conductivity, work function properties and ability for deposition at very thin layers. The degradation of the metal electrode contributes to the overall reduction of cell performance and its origin has been the subject of several recent studies [58].

Two main degradation mechanisms of the metal electrode have been identified; primarily its oxidation at the metal/polymer interface and/or at the upper surface of the metal layer [59] and secondarily its chemical interaction with polymers at its interface with the active layer [60].

The first mechanism, the degradation at the electrode/polymer interface, can result in the formation of an oxidation layer at the metal/polymer interface [61]. This oxidation layer hinders the charge selectivity of the electrode thus reducing device performance. For Ca/Al electrodes it has been reported that their degradation in air is due to considerable changes at the metal–organic interface [59]. Cross-sectional TEM studies have revealed the formation of void structures to be the primary degradation mechanism for Ca/Al contacts. These structures grow as the electrode ages and become oxidized, as shown in Figure 2(a) and (b) [60]. For Ag contacts it has similarly been observed that the electrode becomes oxidized and that an interfacial layer of silver oxide is formed over time, but its formation is a much longer process compared to Al-based electrodes [58].

The second degradation mechanism of the metal electrode, its chemical reaction with the active layer, has also been investigated [7], finding that this mechanism involves the chemical interaction of the thiophenes in the P3HT with the top metal electrodes [60]. For example, Cu electrodes have been found to react with sulfur sites on P3HT during the deposition process [62]. It has also been observed that aluminum penetrates into the active layer, gradually forming aluminum–carbon bonds. A diffused organic–Al interface is formed, which then results in a large oxidized interfacial area upon air exposure. It has been shown that Al interacts with C60, forming Al-C60 bonds that cause reduced charge transport and device performance [63,64].

More recently Jørgensen et al. revealed that aluminum and calcium metal films are highly reactive, but as long as they are kept in an oxygen and water free atmosphere in a glove box environment or encased rigidly, this does not present a problem. In a real world application water and oxygen will always be present and will eventually lead to degradation. The rate of influx or transmission can to a certain extent be controlled by encapsulating the device. Because of the low work function these metals can act as potent reducing agents especially if hydrogen donating reagents like water or alcohols are present. This mode of degradation has not been described yet and the dominant reaction seems instead to be diffusion of water through pores in the metal and reaction to form metal oxides at the interface between the metal and the rest of the device. This metal oxide layer is electrically insulating and creates a transport barrier eventually degrading the performance of the device as seen in the diode characteristics [20]. Glatthaar et al. showed in a series of letters that this layer of Al_2O_3 gives rise to a capacitance that can be estimated from the layer thickness and that changes the standard exponential diode curve to one with an inflection point [65,66]. This may erode the fill factor to a point where the device no longer produces power. Many of the problems with the low work function metal electrodes have been described and interpreted [12], and will also be dealt with in the later sections on oxygen/water degradation in this work.

2.4. Degradation of the hole transport layer

In most OPVs devices, poly (ethylenedioxythiophene) poly (styrenesulfonic acid) (PEDOT:PSS) (Figure 1f and g) is used for the transfer of holes between the transparent electrode and the active layer for normal structures and between the metal electrode and the active layer for inverted structures. Even though the hole transport layer is essential to the efficient function of OPVs devices, the degradation of PEDOT:PSS can shorten the lifetime of the devices. Moreover, the properties of this layer can cause increased degradation of the other layers as well.

However, until now it has been unclear whether the interface between ITO and PEDOT:PSS is stable and which are the parameters that influence its stability. PEDOT:PSS is especially vulnerable to thermal degradation. Even though it has been shown that heat

treatment of PEDOT:PSS films for up to 10–20 min can be beneficial for the electrical properties of the films, prolonged exposure to high temperatures may cause their thermal degradation [67]. Studies of the thermal stability of this material have shown that exposure at 120 °C for over 55 min can significantly reduce its electrical conductivity [68]. In this case, aging was due to the shrinking of the PEDOT conductive grains. However, annealing of PEDOT:PSS films at lower temperatures can help increase their electrical conductivity due to thermal activation of the carriers and improvement of the crystallinity.

The PEDOT:PSS layer is also very sensitive to moisture and oxygen. The detrimental effects of atmospheric air on the electrical properties of this material have been studied [69]. The PEDOT:PSS layer is highly hygroscopic and it was observed that when it absorbs water, its conductivity decreases and consequently device lifetime shortens. It can be observed that the presence of oxygen and moisture promotes the irreversible structural modifications of the PEDOT:PSS chains, reducing its conductivity. The PEDOT:PSS layer can also increase the degradation of other layers of OPVs devices. It has also been observed that water absorbed by the PEDOT:PSS layer can diffuse through the device all the way to the metal cathode accelerating the degradation of the metal electrode and thus reducing device lifetime [70].

Moreover, the PEDOT:PSS layer can increase the degradation of the active layer. Studies on MDMO-PPV/PCBM OPVs have shown that the degradation is associated with water absorption into the PEDOT:PSS layer and charge transport measurements revealed that the effect of water on PEDOT:PSS is to increase the sheet resistance of the PEDOT:PSS/blend layer interface [71]. It has also been reported that the PEDOT:PSS layer can induce the degradation of the active layer in P3HT:PCBM OPVs, which is demonstrated by a decrease in the absorbance and formation of aggregates in the active layer [10]. Recently, it was demonstrated that using processing additives to PEDOT:PSS enhances significantly the hole carrier selectivity in inverted solar cells [72]. Substituting PEDOT:PSS with vacuum deposited MoO_3 as the hole conducting layer enhanced the stability. In a latter more comprehensive study it was found that even in a dry inert atmosphere PEDOT:PSS accelerates degradation presumably due to residual humidity that can diffuse through the device to the cathode interface where it will react [73]. Sputtered nickel oxide (NiO) can also be used as an alternative to PEDOT:PSS with a marked increase in stability [74].

Hancox et al. have found a similar enhanced lifetime of small molecule solar cells with a MoO_x hole-extraction layer [75]. Chromium oxide-chromium nitride films prepared by sputtering have been used by Qin et al. as another alternative to PEDOT:PSS [76].

2.5. Degradation of the electron transport layer

Several n-type materials have been explored as electron transport layer (ETL) in organic solar cells. One of the first was lithium fluoride (LiF) used for energy alignment and stability of the cathode interface [77,78]. Recently, a mixture of C_{60} and LiF has been explored for this purpose in bulk heterojunction solar cells [79,80]. In addition to the enhanced current density the effect of this composite layer was to increase the device lifetime. A number of other types of buffer layers have been introduced for increasing the lifetime of devices with low work function metal electrodes. Sol–gel processed titanium suboxide (TiO_x) can be used, but is a relatively poor conductor in its amorphous form [78,81]. A recent study by Li et al. concluded that TiO_x acts as a photochemically activated oxygen scavenger significantly enhancing the stability of P3HT:PCBM toward both UV exposure and oxygen [82]. Wang et al. have applied thermally evaporated chromium oxide (CrO_x) between the active layer and the aluminum cathode to enhance stability [83]. Wang et al. showed a similar effect for copper oxide (CuO_x) as interface layer either alone or together with lithium fluoride [84]. Wang et al. found that a 1 nm thick layer of lithium benzoate improved both performance and stability [85]. Similarly, the phosphine oxide 2, 7-bis (diphenylphosphoryl)-9, 9′-spirobi [fluorene] has been used to improve the thermo-stability [86]. An early example of using cesium carbonate as a cathode buffer layer was reported [87]. A later comparative study between LiF and Cs_2CO_3 concluded that the latter is superior for enhancing both performance and stability of the devices [88]. Jin et al. have shown that a thin (5 nm) cadmium selenide (CdSe) interface layer retards degradation [89]. Zinc oxide (ZnO) has a high electron mobility and is therefore better suited as an ETL [90]. It is used as an electron transport layer in inverted type devices. The conductance of ZnO is variable and can be modulated by dopants, oxygen vacancies and Zn interstitial atoms [91,92]. In addition it can be changed by exposure to UV-irradiation in the presence of oxygen. This has been exploited in diode devices with memory effects [93]. In solar cell devices this variable conductance can have a dramatic effect where the device has to be pre-treated with exposure to UV-irradiation before full power conversion efficiency is obtained. A chemical mechanism have been proposed [93] and further elaborated by Krebs et al. [94].

A more detailed investigation of the effect of photo annealing of the ZnO layer was carried out [95]. The effect of ZnO electron transport layer in normal geometry devices on the shelf-life have been investigated [96]. The lifetime of devices without any ETL stored in the dark (shelf-lifetime) was very short as opposed to devices with a ZnO nano-particle HTL or mixed ZnO nanoparticles/ZnO sol–gel studied over 78 days. The mixed ETL device proved to be best and retained about 60% efficiency after this period. Transmission electron microscopy cross-sections of the devices showed that voids appeared at the aluminum/P3HT:PCBM interface when no ZnO layer was present. A modification in the form of indium doped zinc oxide nanoparticles (IZO) have been explored in both normal and inverted geometry devices [97]. Sarenpää et al. investigated aluminum doped zinc oxide (AZO) prepared by atomic layer deposition using diethyl zinc and trimethyl aluminum with water as oxygen source. Small molecule devices based on this material showed increased stability with no degradation observed after 40 days [98]. In inverted type devices a thin evaporated layer of aluminum later oxidized to aluminum oxide between the ITO cathode and the PEDOT:PSS layer have been used to enhance electron extraction and in conjunction with a MoO_3 anode interface layer to increase stability [99]. The use of thin evaporated chromium and titanium metal interfaces between the active layer and an aluminum anode has been investigated [100]. With the chromium interlayer superior long-term stability was achieved compared to devices with titanium. For small molecule organic solar cells the influence of various exciton blocking layers on the stability have been investigated [101]. It was found that Alq_3 was superior to In_2S_3, (Z)-5-(4-chlorobenzylidene)-3-(2-ethoxyphenyl)-2-thiox-othiazolidin-4-one (CBBTZ) or bathocuproine (BCP). In addition, it has been found that doping the Alq_3 buffer layer with metallic magnesium enhances the stability even better than for Alq_3 alone [102]. Consequently, the most promising class of materials for hole transport and electrons in the organic bulk heterojunction solar cells are the transition metal oxides.

2.6. Photo-oxidation of the active layer

P3HT:PCBM is a well understood material system that acts as a model for polymer based solar cells. P3HT acts as an electron donor and PCBM as the acceptor. One of the main factors responsible for the degradation of the active layer is the combination of oxygen and light. Hintz et al. reported from their XPS studies that thiophene-based polymers become strongly p-doped upon

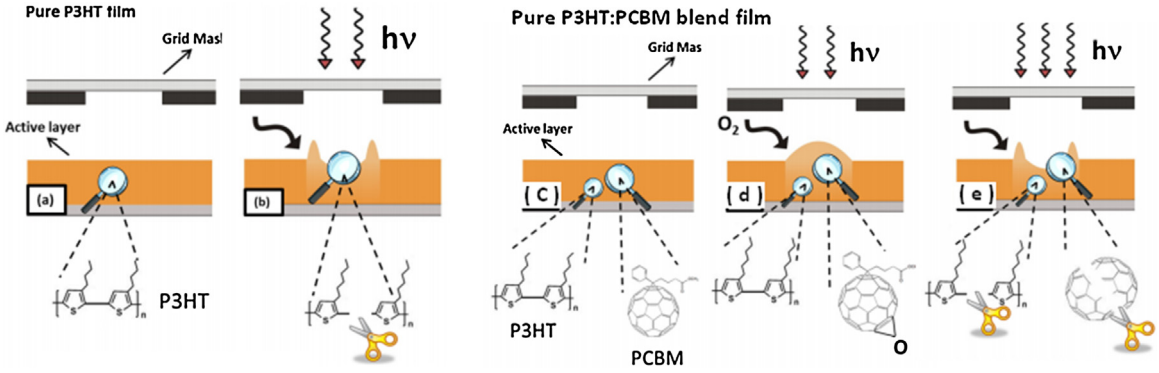

Figure 3. Schematic of the processes occurring inside the pure P3HT layer (a) a zoom into the layer shows intact P3HT chains, (b) on photo-oxidation, the chains get fragmented and evaporate resulting in a decrease in the layer thickness. Schematic of the processes occurring inside the P3HT PCBM blend (C) a zoom into the active layer shows the P3HT and PCBM molecules, (d) on photo-oxidation, incorporation of oxygen into the PCBM results in swelling of the layer, (e) on illuminating the sample for a longer time, the P3HT and the PCBM both get fragmented and evaporate, resulting in the collapse of the layer [53].

interaction with O_2 and light [103]. As a result of this photo-oxidation, fragmentation of the polymers takes place [19] which ultimately results in the evaporation of the material. Abad et al. observed a decrease in the thickness of the active layer made of donor material on photo-oxidation and attributed this to the afore mentioned evaporation [104]. We revealed two competing processes in the blend. Photo-oxidation of PCBM and the fragmentation of P3HT. The fragmentation of the polymer leads to a decrease in the film thickness whereas the photo-oxidation of the fullerene leads to swelling. Other studies on blends suggest that the fast electron transfer from the polymer to fullerene after excitation, accompanied by the formation of polarons on the polymer chain, decreases strongly the reactivity of the polymer against oxygen. This decrease occurs by quenching the triplet formation on the polymer and avoiding a triplet-triplet annihilation reaction with oxygen under formation of reactive singlet oxygen [105]. Lloyd et al. reported that higher charge transfer rate between the donor and acceptor results in lesser photo bleaching and hence less degradation [106]. See Figures 2(c)–(e) and 3 for more understanding on the material fragmentation and evaporation process.

2.6.1. Degradation of PCBM and its effect

Photo-oxidation of the PCBM results in incorporation of oxygen in the fullerene [25]. Studies have been performed on the photo-oxidation of C_{60} molecules previously by Xia et al. where they have reported that interaction between oxygen and C_{60} molecules, induced by irradiation, may occur and can be described as $C_{60} \rightarrow C_{60}O_n + O_2$, $(n = 1–5)$ [107]. Previous attempts at observing photo-oxidation of C_{60} furnished a single monoxide $C_{60}O$ having an epoxide structure [108,109]. Several studies have been done on the oxidation of fullerenes and its derivatives. We will not insist in this work on mechanisms reactionnels but we will reveal the main stages pulled from the literature. The properties of fullerene to trap the radicals by reaction of addition radicalaire lead to the formation of sites radicalaire which can initiate its own degradation. At the first phases of the degradation, the compounds of C_{60} type have been detected [108]. The formation of this molecule results from the addition of an oxygen atom on a double bond of the C_{60} molecule. It forms itself either an epoxide or an oxido-annulene resulting of the isomerization of the epoxide structure. C_{60} compound can evolve toward formation of $C_{120}O$ compounds type [110].

Infrared spectrophotometry has been used for the thermo-oxidation of C_{60} and it is observed of the modifications of the chemical structure which result in the apparition of new absorption strips with increase of the intensity when the temperature increases. This analysis has allowed bringing out the carbonyl products [111]. These defects do not miss to have influence on the properties of the conjugated polymers. It has been brought out in case of PPV, a correlation between the increase of the concentration of carbonyl products and the decrease in the intensity of the photoluminescence. These defects trap the photoluminescence, because the excitons nearest of these defects relax non radiative manner [112]. These defects are responsible of the extinction of the photoluminescence; increase the charge generation [110], because it has been observed an increase of the photocurrent density for samples degraded in relation to virgin samples. As a notable modification of mobility has not been observed, the authors hypothesized that improving of the charge photo-generation would be due to the presence of carbonyl groups which would explain an increase in photocurrent due to the degradation. In summary, we remarked that the oxidizing atmosphere accelerates the degradation process and the oxidation products plays an important role and therefore influence on the characteristics such as charge mobility, trapping excitons, the extinction of photoluminescence and photocurrent.

In addition, PCBM has been observed to stabilize many π-conjugated polymers used in the active layer of organic photovoltaic (OPVs) cells by reducing the degradation rate under different conditions, such as photo-oxidation [25,111,113] and thermolysis [114]. Two mechanisms are usually invoked for the stabilizing effect of PCBM: exciton quenching and radical scavenging. Polymer exciton quenching by electron transfer to PCBM reduces the lifetime of the excited singlet state and thus reduces the population of all reaction-inducing states that are populated via the singlet manifold (e.g., triplet states). Triplet states are notorious for their reactivity, because of their relatively long lifetime, which favors bimolecular reactions such as singlet oxygen sensitization. They recently have been proposed as reactive intermediates in the photo-oxidation of poly (3-hexylthiophene) (P3HT) films [115]. However, the fact that PCBM also drastically reduces the reaction rate of thermolysis of polymers in darkness proves that excited-state quenching is not the only mechanism of stabilization. Chambon et al. have suggested that at least part of the stabilizing effect of fullerenes is due to their ability to scavenge oxygen-centered radicals [114].

On the other hand, PCBM also may accelerate the degradation of some π-conjugated polymers. Because of its high intersystem crossing (ISC) yield, which is 50% in solution [116–118], electronically excited PCBM in the presence of oxygen is well-known for its ability to generate singlet oxygen [119]. In the solid state, the ISC efficiency is much less, but depending on the degree of crystallinity, it might still be high enough to cause significant degradation [120]. Also, superoxide anions have been shown to form by electron transfer from fullerene anions to molecular oxygen [121]. Actually, the increasing degradation rate of a series of polymers in blends with

fullerenes of decreasing electron affinity has been interpreted as a result of enhanced formation of superoxide anions via the fullerene anions [122]. As a further mechanism, triplet energy transfer from the PCBM triplet at 1.57 eV to the polymer triplet state should be possible for most polymers with an optical band gap (S_o–S_1) of less than 2.2 eV (the singlet–triplet splitting (2K) is 0.6–1 eV for most OPV polymers) [123]. The polymer triplet (T_1) may also be populated via recombination of the charge-transfer state (CTS) that is formed in the photoinduced electron transfer reaction at the interface of the polymer and PCBM [124–129]. This triplet recombination will only occur when the CTS is 0.1 eV higher in energy than the polymer T_1 state [130]. (See Ref. [125] for more comprehension.)

2.6.2. Degradation of P3HT

Photochemical degradation of the conjugated polymer and its relation to the overall cell performance has received much attention. Among the mechanisms reported are:

- Photo-bleaching of the polymer which results in a disruption of the π-conjugation.
- Photooxidation, which can lead to disruption of the π-conjugation and/or chain scission. Furthermore, in many cases carbonyl groups are formed that are very efficient exciton quenchers. Due to this quenching many excitons are lost before they can reach the interface with the acceptor prior to their dissociation.
- Photo-doping, corresponding to the (reversible) formation of a weakly bound donor–acceptor charge transfer complex $D + A = [D^{\delta+}A^{\delta-}]$. The latter is an efficient excitation quencher.
- Free radical attack initiated by photolysis of metallic impurities which is usually followed by chain scission and cross-linking [18].

For the bulk polymer it was clearly demonstrated by Manceau et al. that singlet oxygen is most probably the main intermediate responsible for the degradation [19,37]. Based on the identification of degradation products by IR and UV spectroscopy, i.e., carbonyl- and sulfur moieties which come from the degradation of the side chains (α-carbon atom of the hexyl group of P3HT which is the chemically weakest C—H bond) and of the backbone (S-ring) of the polymer, respectively. Manceau et al. list three types of degradation paths: (i) the H abstraction reaction of alkoxy radicals leading to the formation of α-unsaturated alcohol, (ii): the cage reaction of alkoxy radicals with *OH leading to the formation of an aromatic ketone; the latter is unstable when irradiated at wavelengths lower than 400 nm and undergoes a Norrish photolysis, leading to the formation of aromatic carboxylic acid groups and alkyl radicals oxidized into aliphatic acids, and (iii): β-scission leading to the formation of an aromatic aldehyde that rapidly oxidizes into carboxylic acids. Additionally, the S atoms present in the polymer backbone can first are oxidized into sulfoxides, and then to sulfones that decompose into carboxylic acids see (Ref. [19]). The consequences of all these reactions are conjugation loss and/or chain scissions that lead to UV–vis absorbance decrease and hole mobility reduction (the latter being notably due to deep-trap formation) [131].

All this results in efficiency decrease and reduced device operational lifetime. Hintz and his coworkers carried out a systematic study of the influence of environmental factors, namely oxygen, light and moisture, on the photodegradation of neat P3HT [40]. They found out that limited, short-term exposure of the polymer to only one of these degradation triggers only causes small irreversible damage. On the contrary, since P3HT UV-triggered degradation is catalyzed by the presence of H_2O and O_2, exposure of P3HT to for example both UV and oxygen has been found to lead to severe damage of the polymer structure and hence important deterioration of its properties. Interestingly, Hintz et al. evidenced that the lower the P3HT regioregularity, the faster the degradation. Recent studies revealed that, the film thickness of P3HT started decreasing from the beginning of exposure to light and oxygen. This decrease has been attributed to the fragmentation of the polymer and eventually evaporation of the material. This has been verified using NMR spectroscopy by observing a decrease in the signal for the aliphatic part which indicates fragmentation of the hexyl side chains. From the UV–vis data, we observed a decrease in the absorption maxima at 510 nm which indicated the loss of the intact thiophene ring.

As in the case of the photo-degradation, the thermo-oxidation of P3HT causes a progressive decrease of the UV–vis absorbance. This decrease is accompanied of a shift of the maximum toward the weak wavelengths and the disappearance of the wavelengths shoulder. The authors concluded that the thermo-oxidation also leads to the deconjugation. But in the case of the thermo-oxidation, the degradation speed is lower than in the case of the photo-oxidation. IR analysis shows important structural modifications in the P3HT during of the thermal aging. The carbonyl derivatives obtained are identical to those obtained then of the photo-oxidation. However the products detected by IR analysis to 1675 cm^{-1} and 1620 cm^{-1} accumulate in thermo-oxidation, which is not the case in thermo-oxidation. These products are stable thermally and photochemically unstable [19,40].

2.7. Degradation by oxygen and water molecule

Organic materials are sensitive to water and oxygen, so the penetration of these molecules into the device can lead to the deterioration of the active layer [132]. The active layer is usually well protected against atmospheric agents, not only by encapsulation, but also from other layers in the device that act as barriers [133]. However, some water and oxygen molecules can slowly diffuse through the various layers of the device to reach the active layer and react with the polymer materials causing their degradation [134]. The effect of water on the performance of OPV devices has been studied and it has been observed that the presence of moisture within bulk polymers initiates a stronger recombination process, which decreases the ability of charge generation in the bulk heterojunction area [135].

Isotopic labeling and imaging mass spectroscopy have been used successfully in order to map out the oxygen and water process through the various layers of OPV devices. Oxygen [56] and water [136] molecules may diffuse into the device through the metal electrode and permeate through all the layers of the device all the way to the counter (transparent) electrode. Oxygen and water molecules gain entry to the device through microscopic pinholes in the metal electrode [137]. Evidence of the diffusion of water into the device through the aluminum electrode has also been presented for a number of different polymer blends [138,139]. It has also been reported that oxygen molecules are especially harmful to P3HT:PCBM cells under illumination than in dark [7].

2.8. Effect of the atmosphere: organic/metal electrode interface

Several degradation mechanisms are involved during operation of the organic solar cell and each contributes to the overall deterioration of photovoltaic performance that consequently shortens the device lifetime. The most significant contributor is believed to be diffusion of atmosphere into the device of which molecular oxygen and water are known to cause photooxidation of the organic layers and interfaces (chemical degradation), which consequently will disrupt the delicate electrochemical processes that are vital for the photovoltaic performance. Water and molecular oxygen induced photo-oxidation is influenced by various factors that are not necessarily equivalent for both types of atmospheres. Important factors involve: (i) whether or not encapsulation is employed,

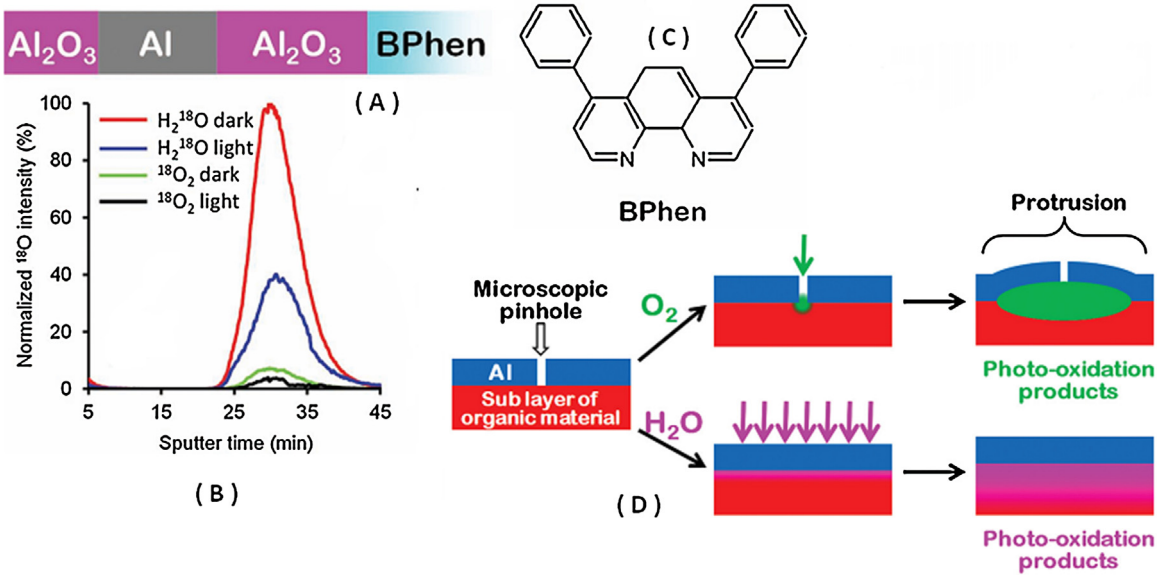

Figure 4. (A) Schematic organic solar cell with the configuration ITO/MeO-TPD:$C_{60}F_{36}$/ZnPc:C_{60}/C_{60}/BPhen/Al showing the BPhen/Al interfaces. (B) The corresponding TOF-SIMS oxygen depth profiles for various experimental conditions. (C) The chemical structure of 4,7-diphenyl-1,10-phenanthroline (BPhen) [140]. (D) Schematic representation of the outer aluminum electrode showing the two different entrance channels for water and molecular oxygen. The molecular oxygen mainly diffuses through microscopic pinholes and water mainly diffuses in between the aluminum grains [20].

and if it is, the type/quality of the encapsulation, (ii) the barrier effect of the individual layers toward molecular oxygen and water, which, among other things, is linked to the individual layer thickness, (iii) and finally the layer stack configuration is important since it will define the accumulated barrier effect at a given location in the device, which could be at an interface or in the bulk of an organic layer. The numerous parameters of which many are interrelated will determine how significant a degradation mechanism is at a specific location in the device [20].

The organic/metal electrode interface is vulnerable toward molecular oxygen and water. Three photo-oxidative degradation mechanisms can take place: (i) as mentioned earlier low work function electrodes such as aluminum and calcium can form metal oxides in the interface that consequently will act as a transport barrier causing deterioration of the photovoltaic performance, (ii) photo-oxidation of the organic material that will degrade the electron/hole transport properties and thus the photovoltaic performance, and (iii) the metal can form an adduct with the organic material that will react efficiently with molecular oxygen and water. However, the latter mechanism has so far not been documented. There are several examples in the literature that demonstrate how powerful it is to combine time-of-flight secondary ion mass spectrometry (TOF-SIMS) with isotopic labeling in order to study water and molecular oxygen induced photo-oxidation of organic solar cells [140–142]. Hermenau et al. employed TOF-SIMS in combination with isotopically labeled atmospheres such as $H_2{}^{18}O$ and $^{18}O_2$ to study photo-oxidation in specific device locations in a non-encapsulated small-molecule organic solar cell with the configuration ITO/MeO-TPD:$C_{60}F_{36}$/ZnPc:C_{60}/C_{60}/BPhen/Al [140]. The authors performed TOF-SIMS depth profiling through the BPhen/Al interface and were able to semi-quantify the formation of aluminum oxide in the interface for various experimental conditions during the device lifetime (Figure 4(A)–(C)).

Hermenau et al. observed that water is significantly worse than molecular oxygen [140]. However, the authors furthermore observed that illumination impedes the aluminum oxide formation at the BPhen/Al interface for both atmospheres, which was ascribed to a temperature effect, i.e., illumination heats up the outer aluminum surface resulting in a lower concentration of molecules from the atmosphere.

Photo-oxidation of the organic material in the organic/metal electrode interface has been described for different types of organic solar cells [140,142]. For evaporated aluminum electrodes a distinct difference in diffusion dynamics is observed for water and molecular oxygen. The phenomenon is schematically described in Figure 4(D).

Water reaches the organic/metal electrode interface by preferentially diffusing in between the aluminum grains, and molecular oxygen preferentially diffuses through microscopic pinholes [142]. Water will thus result in homogeneous photo-oxidation of the organic material in the interface and molecular oxygen will result in inhomogeneous photo-oxidation in the lateral plane; photo oxidation will be centered on the microscopic pinholes causing circular degradation in the lateral plane. As a consequence of the photo-oxidation the organic material will expand in all directions, which for molecular oxygen is manifested as electrode surface protrusions centered on the pinholes. Such protrusions have been measured using interference microscopy and AFM [141]. In the study by Hermenau et al. TOF-SIMS imaging was utilized to visualize this phenomenon for the BPhen/Al interface [140] (Figure 5A and B).

The authors found the corresponding $CN^{18}O$ image for the $^{18}O_2$ exposed device to be equivalent with the ^{18}O image, which they took as evidence that it was the nitrogen part of the molecule (Figure 4(A)–(C)) that was photo-oxidized. The phenomenon shown in Figure 5A and B has been mentioned by Hermenau et al. [140,141]. In several of publications where TOF-SIMS was used in combination with isotopically labeled atmospheres. The circular oriented degradation pattern caused by molecular oxygen has been observed using techniques such as fluorescence microscopy [141], electroluminescence imaging (ELI) [143], photoluminescence imaging (PLI) [143], and light beam induced current microscopy (LBIC) [144]. The obvious way to avoid or diminish this phenomenon is to use thicker electrodes and/or encapsulation.

As mentioned previously the likelihood of water or molecular oxygen reaching a particular location in the device is influenced by

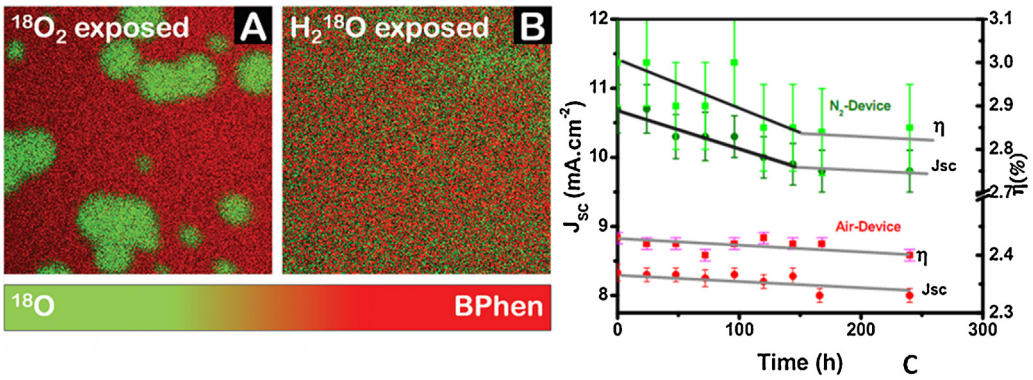

Figure 5. TOF-SIMS composite ion images (500 μm × 500 μm) showing the relative distribution of ^{18}O and BPhen in the BPhen/Al interface for (A) an $^{18}O_2$ exposed device and (B) a $H_2{}^{18}O$ exposed device with the configuration ITO/MeO-TPD:$C_{60}F_{36}$/ZnPc:C_{60}/C_{60}/BPhen/Al [140]. (C) Variation of J_{SC} (circles) and η (squares) of the unencapsulated devices during the aging in the dark [53].

various factors. From the previous examples it is clear that different types of organic solar cells have different vulnerabilities toward water and molecular oxygen.

2.9. Parameters affected and the possible causes

We presented in this section, the correspondence between the main OPVs degradation pathways and their impact on the main characteristics of OPVs cells.

- The fill factor FF is the ratio of the maximum extractable power to the maximum theoretical power output.
  - Reduced interfacial charge transfer efficiency between the different layers (e.g., degradation of the quality of the PAL/electrode interface).
- The serial resistance, R_S, which is notably due to the resistivity of all materials of the OPVs stack, the resistivity of the metallization (such as the busbars), as well as by the contact resistance between the various materials (especially at the PAL/electrode interface).
  - Deterioration of charge transport in the layers (e.g., bulk material degradation).
- The shunt resistance, R_{sh}, which generally reflects the degree of leakage current through the whole device, and which is often linked to imperfections during the production process.
  - Presence of shunts and shorts.
- The open circuit voltage, V_{OC}, is mainly determined by the energy difference between the HOMO of the electron donor and the LUMO of the electron acceptor (E_{gap}). It is also a function of other parameters, such as the temperature.
  - Reduction of the PAL: electrode interface,
  - Lowering of the 'effective' band gap of the PAL blend materials,
  - Electrode Wf change, presence of shorts.
- J_{SC} – light absorption efficiency η_A
  - Chemical degradation of the electron donor (loss of polymer conjugation) of the PAL
- Molecular architecture of the polymer (= band gap) Thickness of the photoactive layer (PAL)
  - Loss of transparency of the stack through which the photon must travel to reach the PAL
- J_{SC} – exciton dissociation efficiency η_{AD}Match of band gap (HOMO (electron acceptor A)/LUMO (electron donor D) levels); D/A blend morphology.
  - Decrease of the D/A interface area/increase of the blend domains (above the diffusion length of the exciton)
- J_{SC} – Carrier (transport and) collection efficiency η_{CC}
  - Loss of percolating paths due to blend reorganization
  - Degradation of the electrode/PAL interface due to for instance electrode degradation
  - Change in energy levels of the cell components
- Percolation pathway to electrodes (D to hole collecting electrode and A to electron collecting electrode)
  - Cracks
- Organization of transportation pathways of the A and of the D materials (e.g., crystallinity)
  - Layer delamination
- Device architecture (e.g., electrode-PAL A/D blend interface area)
  - Degradation of material leading to decrease of charge carrier mobilities/formation of traps.

In definitive, the degradation affects the electrical parameters, opto-electronics, mechanical and induces a decrease/loss in performance of the devices [18].

2.10. Stability of the solar cells

The stability of the organic photovoltaic devices is a concern of critical relevance to the optimization of polymer–fullerene BHJ solar cells. Stability can be assessed in regard to a variety of different parameters including, in particular, ambient and thermal stability [145]. While ambient stability may be realized through encapsulation to protect devices from the action of oxygen and water, thermal stability is a critical issue that currently plagues organic BHJ solar cells [146]. In particular, in devices such as photovoltaic cells, longer periods of time under sunlight exposure result in a temperature increase of the photoactive materials. It has been shown that the phase-instability of MDMO-PPV/PCBM solar cells renders them unstable to long-term exposure to elevated temperatures [147]. Devices based on P3HT/PCBM show better thermal stability because of the inherently greater miscibility of the two components [148]. We have focused more in this section on the ambient stability. As we know, several results unfortunately support the fact that organic barrier films are not 100% efficient with respect to preventing diffusion of water and molecular oxygen through the barrier.

Regarding the barrier and substrate, the main degradation mechanisms occurring are linked to the polymeric nature of the materials used and can lead to a loss of flexibility (because of an increase of stiffness due to polymer aging accelerated by light, moisture and heat). This can ultimately lead to cracks and/or delamination and/or yellowing of the polymer (caused by light, heat and moisture, and which leads to a decrease of photon absorption). Prevention of water and oxygen ingress is generally achieved by the use of a barrier which impedes oxygen and water ingress into the

OPV stack, optionally combined with plastic films containing UV filters.

2.10.1. Barrier effect

As mentioned previously the likelihood of water or molecular oxygen reaching a particular location in the device is influenced by various factors. From the previous examples it is clear that different types of organic solar cells have different vulnerabilities toward water and molecular oxygen. Madsen et al. describes accumulated barrier effects with respect to water and molecular oxygen for a polymer solar cell [142].

The authors used TOF-SIMS in combination with isotopically labeled water and molecular oxygen on a device with the configuration glass/ITO/ZnO/P3HT:PCBM/PEDOT:PSS/Ag/encapsulation together with partial devices. They were able to semi-quantify the incorporation of ^{18}O on the ZnO surface after layer removal, which they used as a measure for the accumulated barrier effect of the layers situated on top of the ZnO layer. For a molecular oxygen atmosphere they observed a steady decrease in oxygen uptake on the ZnO surface for an increased number of layers. However, for the water atmosphere, Madsen et al. observed a drastic decrease for just one layer (P3HT:PCBM) and an equally low level for the subsequent layers, which they ascribed to a bottleneck effect of the P3HT:PCBM layer, which thus must be a relatively good barrier for water. A slightly elevated increase of ^{18}O incorporation was observed for the complete device illuminated in an $H_2{}^{18}O$ atmosphere, which they suggested could be due to the binder being hygroscopic [20,142].

2.10.2. Physical stability: encapsulation

The encapsulation acts as an UV filter removing the most harmful part of the solar spectrum. Due to the organic solar cell sensitivity toward oxygen and water it has been natural to encapsulate them in various ways. This also increases the mechanical stability and scratch resistance [20]. The quality and type of encapsulation play an important role in the stability and overall lifetime of the device by limiting the amount of oxygen and water molecules that permeate the device as well as preventing UV exposure through the utilization of UV filtering encapsulation. UV-blocking layers can increase the long term stability of organic solar cell devices by filtering out UV radiation [149]. In P3HT:PCBM devices with a normal architecture, TiO_2–SiO_x layers have been successfully used to block UV radiation. In the same work, a luminescent layer was also inserted on top of the UV-blocking layer in order to enable photon recycling, thus enhancing device performance [150]. Several encapsulation studies over the past few years have shown that the shelf life of OPVs can be extended to many thousand hours using appropriate encapsulation materials, both flexible and rigid [151,152]. One of the simplest packaging options available is to cover the device with glass plates and use an epoxy-type sealant to hold them in place [153]. This configuration provides effective protection against oxygen and moisture to the device, but is not suitable for the production of flexible devices. Since flexibility is one of the key advantages of OPVs [154].

Several research efforts are focused on developing an encapsulation material that will be flexible and at the same time have all the above advantages: adequate protection to the device, transparency and low-cost. Thin oxide films such as TiO_2 and Al_2O_3 have also been used, although these films are still permeable to some degree by water molecules, mainly due to pinhole defects or to the existence of pores on their surface [155]. Al_2O_3 films deposited by atomic layer deposition (ALD) have been used, either on their own, or in combination with a UV sealant for pentacene-C60 based solar cells [156]. The single Al_2O_3 layer was found to be the most effective sealant, preventing cell degradation to a large degree only 6% loss after over 6000 h of exposure to ambient (but not accelerated) atmospheric conditions. More recently, ultrathin Al_2O_3 layers have been used as encapsulation barriers for P3HT:PCBM OPVs, deposited by a different ALD method [157]. In this study, H_2O has been replaced with O_3 as the ALD oxidant and it has been shown that the Al_2O_3 layers deposited using O_3 displayed superior device encapsulation compared to the films deposited using H_2O and retained 80% of their efficiency after 500 h in air.

Cros et al. used identical conditions for barrier measurements of water uptake and for lifetime measurements of electrical parameters of both normal and inverted type organic solar cells. This allowed them to link the amount of water in contact with the devices and the decrease in performance [158]. This could be used to assess different types of barrier materials such as simple PET or multi layer combinations PE/EVOH/PE or PP/PVA/In/PE. A main conclusion was that to obtain device life-times of several years a water transmission rate of 10^{-3} g m^{-2} day^{-1} was required which is favorable compared to the requirements for OLEDs (10^{-6} g m^{-2} day^{-1}).

There are many different materials that can be used to encapsulate OPVs and they vary considerably in both effectiveness and cost. Since OPV stability is directly related to the temperature, the RH percentage, the periodicity of handling, as well as the spectral distribution of the light source used, standardizing these testing parameters appears crucial. A deeper understanding of the degradation parameters is required to provide material design rules and device engineering concepts toward low-cost and long-lived flexible OPVs.

3. Results and discussion

Exposure tests have been effected in an ambient atmosphere at Mons in Belgium and Abomey-Calavi in Benin. Belgium is situated between 49th and 52nd parallel, halfway between the North Pole and the Equator. A maritime temperate zone: it suffers neither extreme cold nor of the extreme heat (average temperature is 9.4 °C). It does not mean that Belgium is never exposed to harsh weather conditions. As all countries of temperate zone, these meteorological variations are dailies and its four contrasted seasons. Benin is located between latitudes 6° and 12°30 N and longitudes 1° and 4° E, presents at south a subequatorial climate with two rainy seasons and two dry seasons. At north the climate is Sudanese with a moist season and a dry season. At south the average annual pluviometric decreases from Porto-Novo (1200 mm) to Grand-Popo (820 mm). The average monthly temperature varies from 20 °C to 34 °C. At north the temperatures are high and the rainfalls are weaker between 890 and 700 mm except on the Atacora massive which receives on average 1300 mm in Natitingou [53]. The test used are extracted from the aging tests various of the protocols in different conditions: (i) Dark aging test for unencapsulated cells manufactured in air or in an inert atmosphere, (ii) Light aging test (Accelerate Lifetime Test – ALT) of cells manufactured under atmosphere, (iii) Aging test on cells manufactured under ambient atmosphere but encapsulated. The characterization parameters: the open circuit voltage (V_{OC}), the short-circuit current density (J_{SC}), the fill factor (FF), the serial resistance (R_{SA}), the Shunt resistance (R_{sh}) and the energy conversion efficiency (η) are systematically and collectively measured and their evolution according to the different aging tests in the different regions of exposure have been analyzed.

3.1. Dark aging test

Using experimental data, we have meticulously analyzed and interpreted the influence of the manufacturing environment on the devices degradation mechanism. These devices have been subjected to aging to an ambient air but in the dark. During the duration of the experimentation which is 250 h, the temperature has varied from 20 °C to 24 °C and the relative humidity of the

ambient atmosphere from 48% to 5912% (Belgium) [53]. Figure 5C shows two stages in the degradation process for devices manufactured under nitrogen and one for those manufactured in air. The first stage of about 150 h presents a rapid degradation; it is followed by a second stage during which the process is much slower and is spread out in the duration. We remark a decrease of (J_{SC}) and (η) as a function of exposure time for the two series of devices. These devices deteriorate whatever the depositional environment and annealing under nitrogen or under ambient atmosphere. Similar analyzes have been reported in the literature on such a degradation process in two stages [70]. We attribute this rapid degradation which appears at the beginning of the process at chemical modifications at the interface between the cathode and the active layer. The degradation speed appears more important in the first phase for devices manufactured under inert atmosphere by comparison to devices fabricated in air. This result would be due to exposure of cathode interface active film to the degrading elements (O_2, H_2O) during the manufacturing process itself. The devices manufactured in air already evolve in the second stage where degradation is slower. Conversely, the devices manufactured under nitrogen find oneself them, at the beginning of the aging process and therefore an initial rapid degradation mechanism linked to the cathode/active layer takes place first, followed by a second slower [70,159,160]. However, contrary to (J_{SC}) and (η), open circuit voltage (V_{OC}), fill factor (FF) and Shunt resistance (R_{sh}) have not vary on the experimentation period in the same conditions, in accordance with the analysis at $t = 0$. In effect during exposure of the films in the dark but in air, the progressive oxidation of P3HT causes the decrease of conjugation or introducing impurities [136]. This oxidation mechanism leads to the opening of the thiophene ring, causing a decrease in the conjugation and therefore the absorbance in the visible. This mechanism is proposed by Abdou et al. based on the identification of characteristic infrared bands of the products formed.

3.2. Influence of climate

3.2.1. Evolution of (J_{SC}) and (R_{SA}) of the reference structure

These devices are manufactured in ambient atmosphere in Belgium and sealed under nitrogen to avoid all previous degradation, notably during the time of the transport toward the Benin. The devices went out of their packaging at Benin and Belgium at $t = 0$. The measurements effected have showed a stability of (J_{SC}) and (R_{SA}) under nitrogen beyond 240 h in the dark and safe from oxygen and water vapor, which are the main factors of degradation (Figure 6). The very weak decrease of the efficiency (about 5%) remarked for this reference device is attributed to the short periods of exposure to air under simulator during measurements. The reference devices manufactured in air are retained under nitrogen between two measures of parameters under simulator. This experience has enabled us to neglect all processes of degradation during the transport of the devices toward Calavi for the measures in tropical climates [53].

3.2.2. Devices exposure in air and in the dark

Figure 7 shows the evolution of (J_{SC}) and (R_{SA}) during the exposure test in air and in the dark of the devices in Belgium (temperate climate) and to Benin (tropical climate). The decrease of the J_{SC} value as a function of the time is more pronounced for devices exposed in sub-equatorial climate than those exposed under temperate climate for the same period. The exposure under air in the dark during 240 h gives a decrease of (J_{SC}) about 20% for the device tested in Belgium and 33% for those in Benin. During the analysis period, the temperature and humidity respectively varied between 21 °C and 25 °C (21–35 °C) and between 48% and 59% (60–79%) in Belgium (in Benin). We remarked that the accentuation of the decrease of J_{SC} in Benin could be attributed to the

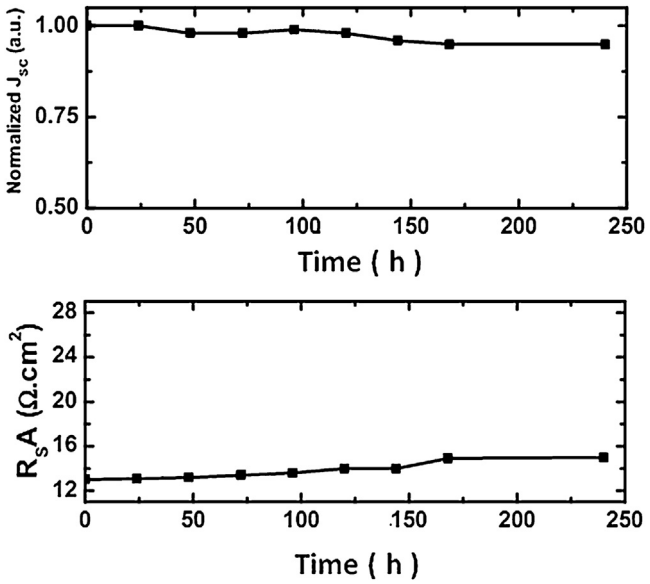

Figure 6. Evolution of (J_{SC}) and (R_{SA}) of the reference structure [53].

contribution of moisture in the devices degradation processes. In the devices structure, the PEDOT-PSS layer serves to the transport and to collect the holes at the anode. Numerous studies in the literature have shown, however, the contribution to the degradation mechanism of water absorbed by the PEDOT-PSS layer due to its hygroscopic character. Once absorbed, water diffuses into the active layer and contributes to the degradation of the electrical properties of the film active/cathode interface. This translated itself by an increase in the serial resistance because the PEDOT-PSS layer becomes less conductive [8]. Some authors esteem that the exposure to moisture accelerates the oxidation of the cathode at the interface with the active layer [11,19,161]. These combined effects hinder the collecting of charges at the electrodes, which induces the decrease in the value of J_{SC} observed for exposed devices in a relative humidity environment more higher. The coherent variations of R_{SA} are observed. R_{SA} increases with time for the exposure to moisture. Whatever the environment, the relative variations of RSA (30% for the exposure to air in Belgium and 92% for the exposure in light in Benin) are more pronounced than those of J_{SC}. The identification of supplemental degradation mechanisms to those described previously and solely related at the charge transport is necessary.

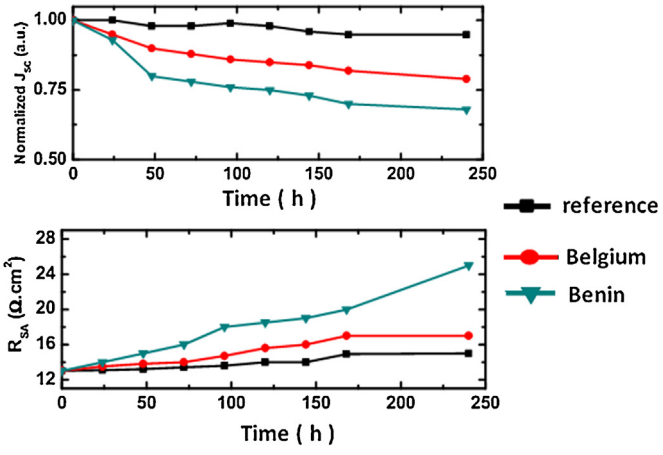

Figure 7. Evolution of (J_{SC}) and (R_{SA}) during the exposure test under air and in the dark [53].

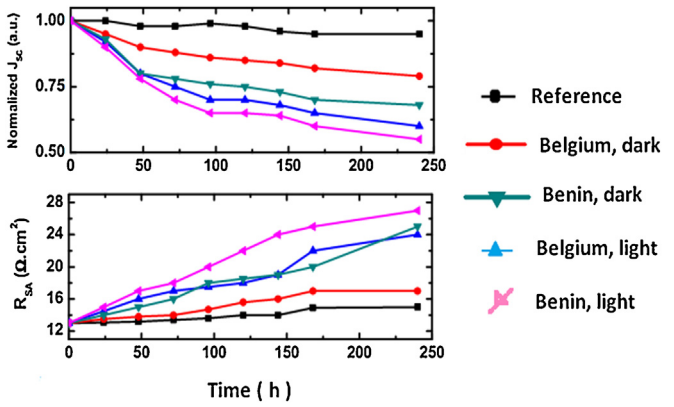

Figure 8. Evolution of (J_{SC}) and (R_{SA}) during the exposure test in ambient air and in the light [53].

3.2.3. Devices exposure in air and in the dark

Figure 8 presents the contribution of the devices exposure to the visible light and the ambient air in the degradation process of those organic films. For all devices, we remarked a decrease of J_{SC} and conjointly the increase of R_{SA} as a function of exposure time. The decrement rate on 240 h of J_{SC} is 40% in Belgium and 45% in Benin. This result shows that the exposure under the light accelerates the aging of the devices independently of exposure climate. The incorporation of species (H_2O; O_2) through the layers is more rapid when the temperature is high (case of Benin), and when the cell is irradiated. The direct consequence is an accelerated loss of the devices properties.

The polymer of the active layer and the PEDOT-PSS layer are all both susceptible to deteriorate under the effect of light. It may occur a desulfonation of the PSS in the presence of water under irradiation because of the acidic environment of the molecules [56,162]. We remarked that the film absorption spectrum of P3HT:PCBM1:0.7 before and after two weeks aging in air and in the dark or in the light is reduced, with an intensification of the process for the film exposed to light. The increased degradation of the absorption is explained by the photo-oxidation of the P3HT donor in the film exposed to air under the light. Oxygen induced the oxidation mechanisms, the chains scission and the formation of defects along the chains (carbonyl groups) which decrease the conjugation length and cause a decrease of the absorption. These different results obtained are due to the oxidation of the hexyl radical and the thiophene ring, which are considered as the photo-oxidation sites of P3HT which have been experimentally studied by many works.

3.2.4. Stability

In this work, these degradation studies have been effected essentially on the unencapsulated solar cells in order to identify the intrinsic mechanisms that induce the loss of optical and electrical properties of the devices.

It appears clearly that the alumina layer deposited forms an effective barrier at the degradation factors in general, and mainly water and oxygen. We have observed however that the degradation process into two phases identified and explicited above appears after all for the encapsulated devices. This encapsulation method is therefore incomplete; which shows that the extrinsic defects play a determinative role on the final quality of the alumina (Al_2O_3) deposits.

Even after encapsulation, the rapid drop of the performances from the first hours of exposure to light is revealing of a first phase of degradation due to the interfaces electrical degradation as described previously. Then, with the encapsulation, the degradation of the second phase is clearly slowered or even suppressed.

It is important to emphasize that most of the degradation mechanisms reviewed here are common to many organic materials and will take place, regardless of the specificities of the material used. Of course, these degradation mechanisms may differ from one system to another to which extent they occur.

At all levels of the stacking, cracks and/or delamination between layers can occur. These phenomena are triggered by mechanical stress. Interfacial stability remains an issue, although it can be manipulated and improved to a certain extent by careful material selection and combination, by tuning the deposition conditions and the thickness of the different layers, as well as by using different device stacks. In fact, interfacial phenomena may occur subsequently to relatively small/short contacts with degradation triggers, which mean that a limited degree of degradation can have a profound impact on the overall performance of the device.

It remains relatively unclear to which extent OPV cells and modules should be resistant toward degradation and which degree of degradation is acceptable to guarantee a specific lifetime.

4. Conclusion

We compared the degradation process in organic bulk heterojunction devices: ITO/PEDOT:PSS/rrP3HT:PC70BM (1:0.7 weight ratio)/Yb/Al, upon exposure to a temperate (Belgium), and subequatorial (Benin) climate. The differences in the degradation process have been studied. The weak performance observed in time for these devices, in terms of electrodes degradation, interfaces and the charge transport mechanism have been analyzed and interpreted. The different studies led on the comparison of the performances and of aging of the unencapsulated devices under various exposure atmospheres (moisture, oxygen, light, darkness) effected in temperate and tropical environments revealed two different stages in the degradation mechanism. A rapid first phase characterized by a decrease of photocurrent and efficiency. This first rapid degradation mechanism is attributed to oxidation of interfaces and an alteration of the charges collection process. A second phase slower is induced by the oxidation of the active film, namely a decrease in the absorption and a degradation of the charge transport process. The diffusion of water through the active layer, the sensitivity of the different layers and interfaces of the device to oxygen (oxidation). These phenomena are more strengthened by the light exposure (photo-aging).

The conjunction of oxygen and light appears very unfavorable and the humidity rate in sub-equatorial climate induces again to the degradation of properties. The decrease of the photovoltaic conversion efficiency is due to the degradation of the absorption and the charge transport properties.

In definitive, it clearly appears that for the overall stability of organic photovoltaic devices, the actual photoactive layer, as well as the properties of the barrier and substrate (e.g., cut of moisture and oxygen ingress, mechanical integrity), remain critical. Interfacial stability is also crucial, as a modest degradation at the level of an interface can quickly and significantly influence the overall device properties.

For future work, we orient our research toward the study of new polymers which shall be adapted to sub-equatorial climate to ensure a stability of the photovoltaic devices.

Acknowledgements

We thank Professor. Jean CHABI OROU-BIO, M.C. Basile. KOUNOUHEWA, Dr. Aristide AKPO, Dr. M. Ossénath, Dr. K. N'GOBI Gabin, Dr. AGBAZO Médard, Dr. ESSOU Adébayo Louis, and Julien Djossou for reading the manuscript. We acknowledge the financial supports by the Trading Company SOCOMAH-Bénin (Isac. T. Madogni), 'Ecole Doctorale Sciences des Matériaux (EDSM)' and

'Laboratoire de Physique du Rayonnement LPR, FAST-UAC 01BP 526 Cotonou République du Bénin'.

References

[1] V. Turkovic, S. Engmann, D.A.M. Egbe, M. Himmerlich, S. Krischok, G. Gobsch, H. Hoppe, Sol. Energy Mater. Sol. Cells 120 (2014) 654.
[2] M.A. Green, K. Emery, Y. Hishikawa, W. Warta, E.D. Dunlop, Prog. Photovolt. Res. Appl. 20 (2012) 12.
[3] Heliatek Press Release, Heliatek Consolidates its Technology Leadership by Establishing a New World Record for Organic Solar Technology with a Cell Efficiency of 12%, 2013, Available at: http://www.heliatek.com/newscenter/latest_news/neuer-weltrekord-fur-organische-solarzellen-heliatek-behauptet-sich-mit-12-zelleffizienz-als-technologiefuhrer/?lang=en.
[4] Q.L. Song, M.L. Wang, E.G. Obbard, X.Y. Sun, X.M. Ding, X.Y. Hou, C.M. Li, Appl. Phys. Lett. 89 (2006) 251118.
[5] S. Schäfer, A. Petersen, T.A. Wagner, R. Kniprath, D. Lingenfelser, A. Zen, T. Kirchartz, B. Zimmermann, U. Würfel, X. Feng, T. Mayer, Phys. Rev. B 83 (2011) 165311.
[6] C. Deibel, V. Dyakonov, Rep. Prog. Phys. 73 (2010) 096401.
[7] E.B.L. Pedersen, T. Tromholt, M.V. Madsen, A.P.L. Böttiger, M. Weigand, J. Mater. Chem. 2 (2014) 5176.
[8] F.C. Krebs, S.A. Gevorgyan, J. Alstrup, J. Mater. Chem. 19 (2009) 5442.
[9] S.A. Gevorgyan, M. Jørgensen, F.C. Krebs, Sol. Energy Mater. Sol. Cells 92 (2008) 736.
[10] M. Manceau, A. Rivaton, J.L. Gardette, S. Guillerez, N. Lemaitre, Sol. Energy Mater. Sol. Cells 95 (2011) 1315.
[11] K. Norrman, M.V. Madsen, S.A. Gevorgyan, F.C. Krebs, J. Am. Chem. Soc. 132 (2010) 1688.
[12] F.C. Krebs, M. Jørgensen, K. Norrman, Sol. Energy Mater. Sol. Cells 92 (2008) 686.
[13] M. Manceau, S. Chambon, A. Rivaton, J.L. Gardette, S. Guillerez, N. Lemaître, Sol. Energy Mater. Sol. Cells 94 (2010) 1572.
[14] M. Manceau, E. Bundgaard, J.E. Carlé, O. Hagemann, M. Helgesen, R. Sondergaard, M. Jorgensen, F.C. Krebs, J. Mater. Chem. 21 (2011) 4132.
[15] A. Sperlich, H. Kraus, C. Deibel, H. Blok, J. Schmid, V. Dyakonov, J. Phys. Chem. B 115 (2011) 13513.
[16] M.V. Madsen, T. Tromholt, A. Böttiger, J.W. Andreasen, K. Norrman, F.C. Krebs, Polym. Degrad. Stab. 97 (2012) 2412.
[17] T. Tromholt, A. Manor, E.A. Katz, F.C. Krebs, Nanotechnology 22 (2011) 225401.
[18] N. Grossiord, J.M. Kroon, R. Andriessen, P.W.M. Blom, Org. Electron. 13 (2012) 432.
[19] M. Manceau, A. Rivaton, J.L. Gardette, S. Guillerez, N. Lematre, Polym. Degrad. Stab. 94 (2009) 898.
[20] M. Jørgensen, K. Norrman, S.A. Gevorgyan, T. Tromholt, B. Andreasen, F.C. Krebs, Adv. Mater. 24 (2012) 580.
[21] A. Distler, P. Kutka, T. Sauermann, H.J. Egelhaaf, D.M. Guldi, D.D. Nuzzo, S.C.J. Meskers, R.A.J. Janssen, Chem. Mater. 24 (2012) 4397.
[22] W. Yang, Y. Yao, C.Q. Wu, Org. Electron. 14 (2013) 1992.
[23] D.E. Motaung, G.F. Malgas, C.J. Arendse, J. Mater. Sci. 46 (2011) 4942.
[24] C.J. Brabec, G. Zerza, G. Cerullo, S. De Silvestri, S. Luzzati, J.C. Hummelen, S. Sariciftci, Chem. Phys. Lett. 340 (2001) 232.
[25] M.O. Reese, A.M. Nardes, B.L. Rupert, R.E. Larsen, D.C. Olson, M.T. Lloyd, S.E. Shaheen, D.S. Dinley, G. Rumbles, N. Kopidakis, Adv. Funct. Mater. 20 (2010) 3476.
[26] J. Schafferhans, A. Baumann, A. Wagenpfahl, C. Deibel, V. Dyakonov, Org. Electron. 11 (2010) 1693.
[27] T. Ameri, G. Dennier, C. Waldauf, H. Azimi, A. Seemann, K. Forberich, J. Hauch, M. Scharber, K. Hingeril, C.J. Brabec, Adv. Funct. Mater. 20 (2010) 1592.
[28] A. Aguirre, S.C.J. Meskers, R.A.J. Janssen, H.J. Egelhaaf, Org. Electron. 12 (2011) 1657.
[29] A. Seemann, T. Sauermann, C. Lungenschmied, O. Armbruster, S. Bauer, H.J. Egelhaaf, J. Hauch, Sol. Energy 85 (2011) 1238.
[30] J. Abad, A. Urbina, J. Colchero, Org. Electron. 12 (2011) 1389.
[31] J. Abad, N. Espinosa, R. Garcia-Valverde, J. Colhero, A. Urbina, Sol. Energy Mater. Sol. Cells 95 (2011) 1326.
[32] A. Seemann, H.J. Egelhaaf, C.J. Brabec, J.A. Hauch, Org. Electron. 19 (2009) 1424.
[33] T. Yamanari, T. Taima, J. Sakai, J. Tsukamoto, Y. Yoshida, Jpn. J. Appl. Phys. 49 (2010) 01.
[34] S. Chambon, A. Rivaton, J.L. Gardette, M. Firon, L. Lutsen, J. Polym. Sci. A: Polym. Chem. 45 (2007) 317.
[35] S. Chambon, A. Rivaton, J.L. Gardette, M. Firon, Sol. Energy Mater. Sol. Cells 92 (2008) 785.
[36] S. Chambon, A. Rivaton, J.L. Gardette, M. Firon, J. Polym. Sci. A: Polym. Chem. 47 (2009) 6044.
[37] M. Manceau, A. Rivaton, J.L. Gardette, Macromol. Rapid Commun. 29 (2008) 1823.
[38] M. Manceau, J. Gaume, A. Rivaton, J.L. Gardette, G. Monier, L. Bideux, Thin Solid Films 518 (2010) 7113.
[39] H. Hintz, C. Sessler, H. Peisert, H.J. Egelhaaf, T. Chasse, Chem. Mater. 24 (2012) 2739.
[40] H. Hintz, H.J. Egelhaaf, L. Lüer, J. Hauch, H. Peisert, T. Chassé, Chem. Mater. 23 (2011) 145.
[41] R.D. Scurlock, B.J. Wang, P.R. Ogilby, J.R. Sheats, R.L. Clough, J. Am. Chem. Soc. 117 (1995) 10194.
[42] N. Dam, R.D. Scurlock, B.J. Wang, L.C. Ma, M. Sundahl, P.R. Ogilby, Chem. Mater. 11 (1999) 1302.
[43] L.C. Ma, X.S. Wang, B.J. Wang, J.R. Chen, J.H. Wang, K. Huang, B.W. Zhang, Y. Cao, Z.H. Han, S.P. Qian, S.D. Yao, Chem. Phys. 285 (2002) 85.
[44] M.S. Abdou, S. Holdcroft, Macromolecules 26 (1993) 2954.
[45] M.S.A. Abdou, S. Holdcroft, Can. J. Chem. 73 (1995) 1893.
[46] H. Hintz, H. Peisert, H.J. Egelhaaf, T. Chasse, J. Phys. Chem. C 115 (2011) 13373.
[47] H.H. Liao, C.M. Yang, C.C. Liu, S.F. Horng, H.F. Meng, J.T. Shy, J. Appl. Phys. 103 (2008) 104506.
[48] http://www.risoe.dtu.dk/news_archives/news/2009/0916_solceller_afrika.
[49] http://www.eight19.com/technology/indigo-delivers-power-grid-communities.
[50] C. Waldauf, P. Schilinsky, M. Perisutti, C.J. Brabec, Adv. Mater. 15 (2003) 2084.
[51] F. Monestier, J.J. Simon, P. Torchio, L. Escoubas, F. Flory, S. Baill, R. Bettignies, S. Guillerez, C. Defranoux, Sol. Energy Mater. Sol. Cells 91 (2007) 405.
[52] D.J. Servaites, M.A. Ratner, T.J. Marks, Energy Environ. Sci. 4 (2011) 4410.
[53] M.B. Agbomahéna, Joint Supervision Between UMons, Belgium (Ph.D. thesis), University of Abomey-Calavi, Benin, 2013.
[54] M. Lira-Cantu, K. Norrman, J.W. Andreasen, F.C. Krebs, Chem. Mater. 18 (2006) 5684.
[55] J. Alstrup, K. Norrman, M. Jørgensen, F.C. Krebs, Sol. Energy Mater. Sol. Cells 90 (2006) 2777.
[56] K. Norrman, N.B. Larsen, F.C. Krebs, Sol. Energy Mater. Sol. Cells 90 (2006) 2793.
[57] C.J. Brabec, S.E. Shaheen, C. Winder, N.S. Sariciftci, P. Denk, Appl. Phys. 80 (2002) 1288.
[58] M. Wang, F. Xie, J. Du, Q. Tang, S. Zheng, Q. Miao, J. Chen, N. Zhao, J.B. Xu, Sol. Energy Mater. Sol. Cells 95 (2011) 3303.
[59] M.T. Lloyd, D.C. Olson, P. Lu, E. Fang, D.L. Moore, M.S. White, M.O. Reese, D.S. Ginley, J.W.P. Hsu, J. Mater. Chem. 19 (2009) 7638.
[60] L. Zhao, T.C.W. Mak, Organometallics 26 (2007) 4439.
[61] Y. Dong, Y. Geng, J. Ma, R. Huang, Organometallics 25 (2006) 447.
[62] A. Lachkar, A. Selmani, E. Sacher, M. Leclerc, R. Mokhliss, Synth. Met. 66 (1994) 209.
[63] J. Nishinaga, T. Aihara, H. Yamagata, Y. Horikoshi, J. Cryst. Growth 278 (2005) 633.
[64] M.O. Reese, A.J. Morfa, M.S. White, N. Kopidakis, S.E. Shaheen, G. Rumbles, D.S. Ginley, Sol. Energy Mater. Sol. Cells 92 (2008) 746.
[65] M. Glatthaar, M. Riede, N. Keegan, K. Sylvester-Hvid, B. Zimmermann, M. Niggemann, A. Hinsch, A. Gompert, Sol. Energy Mater. Sol. Cells 91 (2007) 390.
[66] M. Glatthaar, N. Mingirulli, B. Zimmermann, T. Ziegler, R. Kern, M. Niggemann, A. Hinsch, A. Gombert, Phys. Status Solidi A 202 (2005) R125.
[67] J. Huang, P.F. Miller, J.C. de Mello, A.J. de Mello, D.D.C. Bradley, Synth. Met. 139 (2003) 569.
[68] E. Vitoratos, S. Sakkopoulos, E. Dalas, N. Paliatsas, D. Karageorgopoulos, F. Petraki, S. Kennou, S.A. Choulis, Org. Electron. 10 (2009) 61.
[69] E. Vitoratos, S. Sakkopoulos, N. Paliatsas, K. Emmanouil, S.A. Choulis, Open J. Org. Polym. Mater. 2 (2012) 7.
[70] E. Voroshazi, B. Verreet, A. Buri, R. Muller, D. Di Nuzzo, P. Heremans, Org. Electron. 12 (2011) 736.
[71] K. Kawano, R. Pacios, D. Poplavskyy, J. Nelson, D.D.C. Bradley, J.R. Durrant, Sol. Energy Mater. Sol. Cells 90 (2006) 3520.
[72] A. Savva, M. Neophytou, C. Koutsides, K. Kalli, S.A. Choulis, Org. Electron.: Phys. Mater. Appl. 14 (2013) 3123.
[73] E. Voroshazi, B. Verreet, T. Aernouts, P. Heremans, Sol. Energy Mater. Sol. Cells 95 (2011) 1303.
[74] R. Betancur, M. Maymó, X. Elias, L.T. Vuong, J. Martorell, Sol. Energy Mater. Sol. Cells 95 (2011) 735.
[75] I. Hancox, P. Sullivan, K.V. Chauhan, N. Beaumont, L.A. Rochford, R.A. Hatton, T.S. Jones, Org. Electron. 11 (2010) 2019.
[76] P. Qin, G. Fang, Q. He, N. Sun, X. Fan, Q. Zheng, F. Chen, J. Wan, X. Zhao, Sol. Energy Mater. Sol. Cells 95 (2011) 1005.
[77] G. Yu, J. Gao, J.C. Hummelen, F. Wudl, A.J. Heeger, Science 270 (1995) 1789.
[78] J.Y. Kim, S.H. Kim, H.H. Lee, A.J. Heeger, Adv. Mater. 18 (2006) 572.
[79] D. Gao, M.G. Helander, Z.B. Wang, D.P. Puzzo, M.T. Greiner, Z.H. Lu, Adv. Mater. 22 (2010) 5404.
[80] K. Kawano, C. Adachi, Appl. Phys. Lett. 96 (2010) 053307.
[81] C. Waldauf, M. Morana, P. Denk, P. Schilinsky, K. Coakley, S.A. Choulis, C.J. Brabec, Appl. Phys. Lett. 89 (2006) 233517.
[82] J. Li, S. Kim, S. Edington, J. Nedy, S. Cho, K. Lee, A.J. Heeger, M.C. Gupta, J.T. Yates, Sol. Energy Mater. Sol. Cells 95 (2011) 1123.
[83] M. Wang, Q. Tang, J. An, F. Xie, J. Chen, S. Zheng, K.Y. Wong, Q. Miao, J. Xu, ACS Appl. Mater. Interfaces 2 (2010) 2699.
[84] M. Wang, F. Xie, W. Xie, S. Zheng, N. Ke, J. Chen, N. Zhao, J.B. Xu, Appl. Phys. Lett. 98 (2011) 183304.
[85] Y. Wang, L. Yang, C. Yao, W. Qin, S. Yin, F. Zhang, Sol. Energy Mater. Sol. Cells 95 (2011) 1243.
[86] S.O. Jeon, J.Y. Lee, Sol. Energy Mater. Sol. Cells 95 (2011) 1102.
[87] F.C. Chen, J.L. Wu, S.S. Yang, K.H. Hsieh, W.C. Chen, J. Appl. Phys. 103 (2008) 103721.
[88] L. Yang, H. Xu, H. Tian, S. Yin, F. Zhang, Sol. Energy Mater. Sol. Cells 94 (2010) 1831.

[89] H. Jin, M. Tuomikokoski, J. Hiltunen, P. Kopola, A. Maaninen, F. Pino, J. Phys. Chem. C 113 (2009) 16807.
[90] D.C. Olson, S.E. Shaheen, N. Kopidakis, D.S. Ginley, Appl. Phys. Lett. 89 (2006) 143517.
[91] Ü. Özgür, Y.I. Alivov, C. Liu, A. Teke, M.A. Reshchikov, S. Dogan, V. Avrutin, S.J. Cho, H. Morko, J. Appl. Phys. 98 (2005) 041301.
[92] S.J. Pearton, D.P. Norton, K. Ip, J.W. Heo, J. Vac. Sci. Technol. B 22 (2004) 932.
[93] F. Verbakel, S.C.J. Meskers, R.A.J. Janssen, Appl. Phys. Lett. 89 (2006) 102103.
[94] F.C. Krebs, T. Tromholt, M. Jørgensen, Nanoscale 2 (2010) 873.
[95] M.R. Lilliedal, A.J. Medford, M.V. Madsen, K. Norrman, F.C. Krebs, Sol. Energy Mater. Sol. Cells 94 (2010) 2018.
[96] S.R. Ferreira, P. Lu, Y.-J. Lee, R.J. Davis, J.W.P. Hsu, J. Phys. Chem. C 115 (2011) 13471.
[97] A. Puetz, T. Stubhan, M. Reinhard, O. Loesch, E. Hammarberg, S. Wolf, C. Feldmann, H. Kalt, A. Colsmann, U. Lemmer, Sol. Energy Mater. Sol. Cells 95 (2011) 579.
[98] H. Sarenpää, T. Niemi, A. Tukainen, H. Lemmetyinen, N. Tkachenko, Sol. Energy Mater. Sol. Cells 94 (2010) 1379.
[99] H. Zhang, J. Ouyang, Appl. Phys. Lett. 97 (2010) 063509.
[100] B. Zimmermann, U. Würfel, M. Niggemann, Sol. Energy Mater. Sol. Cells 93 (2009) 491.
[101] Y. Lare, B. Kouskoussa, K. Benchouck, S.O. Ouro Djobo, L. Cattin, M. Morsli, F.R. Diaz, M. Gacitua, T. Abachi, M.A. del Valle, F. Armijo, G.A. East, J.C. Bernède, J. Phys. Chem. Solids 72 (2011) 97.
[102] M.F. Lo, T.W. Ng, S.L. Lai, F.L. Wong, M.K. Fung, S.T. Lee, C.S. Lee, Appl. Phys. Lett. 97 (2010) 143304.
[103] H. Hintz, H.J. Egelhaaf, H. Peisert, T. Chassé, Polym. Degrad. Stab. 95 (2010) 818.
[104] H. Antoniadis, L.J. Rothberg, F. Papadimitrakopoulos, M. Yan, M.E. Galvin, M.A. Abkowitz, Phys. Rev. B 50 (1994) 14911.
[105] H. Neugebauer, C. Brabec, J.C. Hummelen, N.S. Sariciftci, Sol. Energy Mater. Sol. Cells 61 (2000) 35.
[106] M.T. Lloyd, A. Garcia, J.J. Berry, M.O. Reese, D.S. Ginley, D.C. Olson, 37th IEEE Photovoltaic Specialists Conference, vol. 6, Seattle, Washington, 2011.
[107] A.D. Xia, S. Wada, H. Tashiro, Appl. Phys. Lett. 73 (1998) 1323.
[108] K.M. Creegan, J.L. Robbins, W.K. Robbins, J.M. Millar, R.D. Sherwood, P.J. Tindall, D.M. Cox, J.P. McCauley, D.R. Jones, J. Am. Chem. Soc. 114 (1992) 1103.
[109] N.P. Curry, B. Doust, D.A. Jelski, J. Cluster Sci. 12 (2001) 385.
[110] R. Taylor, M.P. Barrow, T. Dreuello, Chem. Commun. 56 (1998) 2497.
[111] R. Taylor, A. Penicaud, N.J. Tower, J. Chem. Phys. Lett. 295 (1998) 481.
[112] F. Papadimitrakopoulos, M. Yan, J.L. Rothberg, H.E. Katz, E. Chandross, M.E. Galvin, Mol. Cryst. Liquid Cryst. 256 (1994) 663.
[113] T. Tromholt, M.V. Madsen, J.E. Carle, M. Helgesen, F.C. Krebs, J. Mater. Chem. 22 (2012) 7592.
[114] S. Chambon, A. Rivaton, J.L. Gardette, M. Firon, Sol. Energy Mater. Sol. Cells 91 (2007) 394.
[115] A. Sperlich, H. Kraus, C. Deibel, H. Blok, J. Schmidt, V. Dyakonov, J. Phys. Chem. B 115 (2011) 13513.
[116] F.A. Salazar, A. Fedorov, S.M.N. Berberan, Chem. Phys. Lett. 271 (1997) 361.
[117] F. Prat, R. Stackow, R. Bernstein, W. Qian, Y. Rubin, C.S. Foote, J. Phys. Chem. A 103 (1999) 7230.
[118] H. Wang, Y. He, Y. Li, H. Su, J. Phys. Chem. A 116 (2012) 255.
[119] J.W. Arbogast, A.P. Darmanian, C.S. Foote, Y. Rubin, F.N. Diederich, M.M. Alvarez, S.J. Anz, R.L. Whetten, J. Phys. Chem. 95 (1991) 11.
[120] S. Cook, H. Ohkita, Y. Kim, S.J.J. Benson, D.D.C. Bradley, J.R. Durrant, Chem. Phys. Lett. 445 (2007) 276.
[121] Y. Yamakoshi, N. Umezawa, A. Ryu, K. Arakane, N. Miyata, Y. Goda, T. Masumizu, T. Nagano, J. Am. Chem. Soc. 125 (2003) 12803.
[122] C. Taliani, G. Ruani, R. Zamboni, R. Danieli, S. Rossini, V.N. Denisov, V.M. Burlakov, F. Negri, G. Orlandi, F. Zerbetto, J. Chem. Soc. Chem. Commun. 3 (1993) 220.
[123] A. Kohler, H.H. Bassler, Mater. Sci. Eng. Rep. 66 (2009) 71.
[124] T.A. Ford, I. Avilov, D. Beljonne, N.C. Greenham, Phys. Rev. B 71 (2005) 125212.
[125] T. Offermans, P.A. van Hal, S.C.J. Meskers, M.M. Koetse, R.A. Janssen, J. Phys. Rev. B 72 (2005) 045213.
[126] D. Veldman, O. Ipek, S.S.J. Meskers, J. Sweelssen, M.M. Koetse, S.C. Veenstra, J.M. Kroon, S.S. van Bavel, J. Loos, R.A.J. Janssen, J. Am. Chem. Soc. 130 (2008) 7721.
[127] S. Westenhoff, I.A. Howard, J.M. Hodgkiss, K.R. Kirov, H.A. Bronstein, C.K. Williams, N.C. Greenham, R.H. Friend, J. Am. Chem. Soc. 130 (2008) 13653.
[128] C.D. Smith, L.X. Reynolds, A. Bruno, D.D.C. Bradley, S.A. Haque, J. Nelson, Adv. Funct. Mater. 20 (2010) 2701.
[129] M. Liedtke, A. Sperlich, H. Kraus, A. Baumann, C. Deibel, M.J.M. Wirix, J. Loos, C.M. Cardona, V. Dyakonov, J. Am. Chem. Soc. 133 (2011) 9088.
[130] D. Veldman, S.C.J. Meskers, R.A. Janssen, Adv. Funct. Mater. 19 (2009) 1939.
[131] R. Pacios, A.J. Chatten, K. Kawano, J.R. Durrant, D.D.C. Bradley, J. Nelson, Adv. Funct. Mater. 16 (2006) 2117.
[132] H. Jin, J. Olkkonen, M. Tuomikoski, P. Kopola, A. Maaninen, J. Hast, Sol. Energy Mater. Sol. Cells 94 (2010) 465.
[133] M. Hermenau, S. Schubert, H. Klumbies, J. Fahlteich, L.M. Meskamp, K. Leo, M. Riede, Sol. Energy Mater. Sol. Cells 97 (2012) 102.
[134] G.L. Graff, R.E. Williford, P.E. Burrows, J. Appl. Phys. 96 (2004) 1840.
[135] S.R. Dupont, E. Voroshazi, P. Heremans, R.H. Dauskardt, 38th IEEE Photovoltaic Specialists Conference, Austin, TX, USA, 2012, p. 3259, Art 6318272.
[136] K. Norrman, S.A. Gevorgyan, F.C. Krebs, ACS Appl. Mater. Interfaces 1 (2009) 102.
[137] F.C. Krebs, K. Norrman, Prog. Photovolt. Res. Appl. 15 (2007) 697.
[138] S.A. Gevorgyan, F.C. Krebs, Chem. Mater. 20 (2008) 4386.
[139] V.M. Drakonakis, A. Savva, M. Kokonou, S.A. Choulis, Sol. Energy Mater. Sol. Cells 130 (2014) 544.
[140] M. Hermenau, M. Riede, K. Leo, S.A. Gevorgyan, F.C. Krebs, K. Norrman, Sol. Energy Mater. Sol. Cells 95 (2011) 1268.
[141] K. Norrman, F.C. Krebs, Sol. Energy Mater. Sol. Cells 90 (2006) 213.
[142] M.V. Madsen, K. Norrman, F.C. Krebs, J. Photon. Energy 1 (2011) 011104.
[143] M. Seeland, R. Rösch, H. Hoppe, J. Appl. Phys. 109 (2011) 064513.
[144] M.T. Lloyd, C.H. Peters, A. Garcia, I.V. Kauvar, J.J. Berry, M.O. Reese, M.D. McGehee, D.S. Ginley, D.C. Olson, Sol. Energy Mater. Sol. Cells 95 (2011) 1382.
[145] J.M.J. Fréchet, B.C. Thompson, Angew. Chem. Int. Ed. Engl. 47 (2008) 58.
[146] J.L. Delgado, N. Martın, P. de la Cruz, F. Langa, Chem. Soc. Rev. 40 (2011) 5232.
[147] X. Yang, J.K.J. van Duren, R.A.J. Janssen, A.J. Michels, J. Loos, Macromolecules 37 (2004) 2151.
[148] K. Sivula, C.K. Luscombe, B.C. Thompson, J.M.J. Fréchet, J. Am. Chem. Soc. 128 (2006) 13988.
[149] M.S. Ryu, H.J. Cha, J. Jang, Sol. Energy Mater. Sol. Cells 94 (2010) 152.
[150] S. Engmann, M. Machalett, V. Turkovic, R. Rösch, E. Rädlein, G. Gobsch, H. Hoppe, J. Appl. Phys. 112 (2012) 034517.
[151] C. Lungenschmied, G. Dennler, H. Neugebauer, N.S. Sariciftci, M. Glatthaar, T. Meyer, A. Meyer, Sol. Energy Mater. Sol. Cells 91 (2007) 379.
[152] F.C. Krebs, Sol. Energy Mater. Sol. Cells 90 (2006) 3633.
[153] S. Schuller, P. Schilinsky, J. Hauch, C.J. Brabec, Appl. Phys. A 79 (2004) 37.
[154] M. Kaltenbrunner, M.S. White, E.D. Glowacki, T. Sekitani, T. Someya, N.S. Sariciftci, S. Bauer, Nat. Commun. 3 (2012) 770.
[155] G. Dennler, C. Lungenschmied, H. Neugebauer, N.S. Sariciftci, A. Labouret, J. Mater. Res. 20 (2005) 3224.
[156] W.J. Potscavage, S. Yoo, B. Domercq, B. Kippelen, Appl. Phys. Lett. 90 (2007) 253511.
[157] S. Sarkar, J.H. Culp, J.T. Whyland, M. Garvan, V. Misra, Org. Electron. 11 (2010) 1896.
[158] S. Cros, R. de Bettignies, S. Berson, S. Bailly, P. Maisse, N. Lemaitre, S. Guillerez, Sol. Energy Mater. Sol. Cells 95 (2011) 565.
[159] Y. Gao, Mater. Sci. Eng. Rep. 68 (2010) 39.
[160] A. Sharma, G. Anderson, D.A. Lewis, Phys. Chem. Chem. Phys. 13 (2011) 4381.
[161] X. Wang, C.X. Zhao, G. Xu, Z. Chen, F. Zhu, Sol. Energy Mater. Sol. Cells 104 (2012) 1.
[162] X. Crispin, J. Polym. Sci. B: Polym. Phys. 41 (2003) 2561.